Newhouse sinks in the self-similar bifurcation structure

Binoy Krishna Goswami*
Laser and Plasma Technology Division, Bhabha Atomic Research Centre, Mumbai 400 085, India
(Received 14 January 2000)

The numerical analyses of the dynamics of periodically driven Toda oscillator suggest the following features. Primary Newhouse orbits (sinks and saddles) are born in sequence when the oscillator proceeds through various subharmonic resonance regions. As the control parameter is swept in the neighboring parameter space of the homoclinic tangency for a primary saddle, first order secondary Newhouse sinks are born around the corresponding primary sink in a series of period n-tupling ($n>2$) processes. Higher order secondary Newhouse sinks are similarly born, in a recurrent manner, around those first-order secondary sinks, constituting a self-similar bifurcation structure in the parameter space. Each higher (say nth) order secondary Newhouse sink appears and undergoes sequence of period doubling (before being destroyed by crises), within a small subinterval of the control parameter window where the $(n-1)$th-order secondary Newhouse sink exists. The nth-order secondary Newhouse orbits appear in the basin of the $(n-1)$th-order secondary Newhouse sink. Thus, the higher-order secondary sinks appear with progressively smaller basins intertwined with the basins of lower-order secondary sinks.

PACS number(s): 05.45.Pq, 05.45.Ac, 42.65.Sf, 47.52.+j

A periodically driven nonlinear oscillator exhibits various subharmonic (harmonic) resonances if the driving frequency is multiples of (equal to) the natural frequency of the oscillator. Each period-n resonance ($n \geqslant 1$) gives birth of a period-n saddle node bifurcation. If one changes the value of some suitable system parameter (''control parameter''), a cascade of such resonances may occur, leading to an infinitely large sequence of saddle node bifurcations.[1] The associated nodes later undergo sequence of period doubling, constituting various branches. Some of these branches may even coexist in some intervals on the control parameter axis, leading to multistability. Multistability has been observed in a variety of nonlinear systems, for instance, in electronic circuits [3,4], lasers [5–9], geophysical models [10], mechanical systems [11], and also in some standard models such as Hénon map [12] and Duffing oscillator [13–15]. The number of coexisting states increases if the dissipativity reduces. This has been experimentally observed by Meucci *et al.* [16] in CO_2 laser, and numerically shown in Refs. [17–20] from the laser rate equations [5,7,8,21–23], a well known class-B laser model. Feudel *et al.* [24] have theoretically shown the coexistence of around a hundred periodic sinks at small dissipativity in the case of a two-dimensional map representing a periodically kicked mechanical rotor. A natural question that arises is about the limit of the complex nature of multistability, and about some possible order behind such complexity. Newhouse [25] has predicted about an infinitely large sequence of coexisting sinks in the neigboring parameter space of homoclinic tangency. These celebrated predictions of Newhouse have motivated many groups of researchers [26–30] for thorough investigations, and probably have remained an open subject until today. Laura Tedeschini-Lalli and Yorke [26] have shown that, for an apparently typical situation, Newhouse sinks may occur for a set of parameter values of Lebesgue measure zero. Lai *et al.* [27] have observed that nonhyperbolic chaotic saddles are common in chaotic systems. In the case of Hénon map, Kan *et al.* [28] have shown evidence of persistent homoclinic tangencies, and Grebogi *et al.* [29] have shown that the boundary of a basin (born in saddle node bifurcation) could become fractal after first homoclinic tangency of the corresponding boundary saddle. From the analyses of laser rate equations and Hénon map, Eschenazi *et al.* [30] have shown that the basins are systematically organized in phase space, determined by the ordering of the heteroclinic and homoclinic intersections of the invariant manifolds of the boundary saddles. They have also stated about the birth of secondary Newhouse sinks around the primary Newhouse sinks. However, they have not explored the possible recurrent appearance of similar higher order secondary sinks around these secondary Newhouse sinks. We believe it would be worthwhile to study these directions. If one takes an integrated approach to analyze the birth of periodic orbits in a periodically forced system, such a scenario appears feasible. For instance, let us consider a case when various primary Newhouse orbits are born around the stable period-1, as the system enters through the series of various subharmonic resonances. Next, a series of secondary Newhouse sinks are born around these primary Newhouse sinks, as Eschenazi *et al.* have observed. In such a case, one may expect a similar trend to continue, giving birth to a set of simultaneously coexisting higher-order secondary Newhouse sinks; the number of such sinks depending on the parameter values. We have recently [17,19,20] demonstrated some similar phenomena from the numerical analyses of the Toda oscillator form [18,31,32] of the laser rate equations.

*Email address: bgoswami@apsara.barc.ernet.in

[1]Gavrilov and Shilnikov [1,2] have predicted the birth of an infinitely large sequence of saddle node bifurcations, in the case of diffeomorphisms, close to homoclinic tangency of the invariant manifolds of a ''boundary saddle'' (i.e., a saddle, born in saddle node bifurcation).

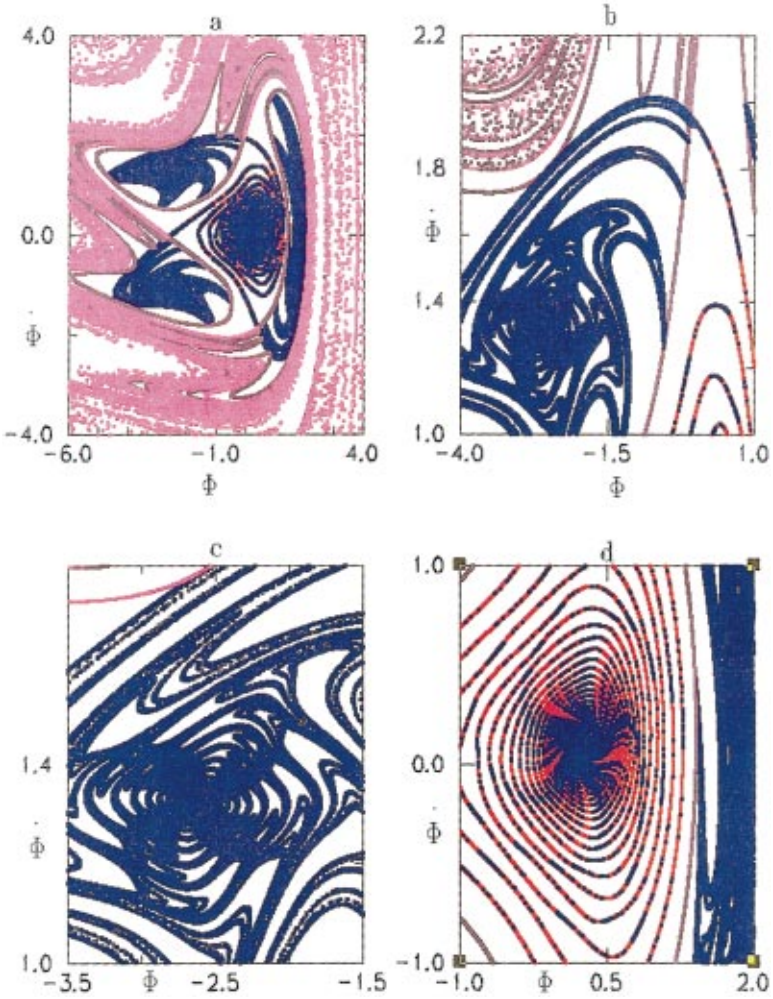

FIG. 1. (Color) Homoclinic tangency of the period-3 manifolds. $\omega=2.5$ and $m=0.00474$. Two components of the unstable manifold are shown respectively by blue and red points. Two components of the stable manifold are shown respectively by maroon and magenta points. The plot (b), a closeup of plot (a), shows more clearly the stretching and folding of the maroon stable component and its eventual accumulation near the magenta stable component. The blue unstable component also undergoes similar stretching and folding while approaching the period-3 sink [at the center of plot (c) where the blue component is dense] and the period-1 sink [at the center of plot (d) where both blue and red components are dense].

We observed the creation of various n-tupled[2] orbits in a self-similar bifurcation structure. We review Ref. [20] to explain the self-similarity of the bifurcation structure in a few lines. In between any two successive bifurcation curves of this structure, one finds a series of bifurcation substructures, born in various processes of n tuplings. For instance, in between two successive period doubling bifurcation curves (say $m/2\rightarrow m$ and $m\rightarrow 2m$), the substructure, born in period tripling, will have a boundary of period-$3m$ saddle node bifurcation curve, and a sequence of period doubling ($3m\times 2^{l-1}\rightarrow 3m\times 2^{l}$; $l=1,2,3,\ldots$) bifurcation curves within the boundary. Similarly, the substructure, born in period quadrupling, will have a boundary of period-$4m$ saddle node bifurcation curve, and a sequence of period doubling ($4m\times 2^{l-1}\rightarrow 4m\times 2^{l}$; $l=1,2,3,\ldots$) bifurcation curves within the boundary. Such a process occurs in a self-similar manner within these bifurcation substructures, giving birth of fine and hyperfine structures. Since, in each of these n-tupling processes, the original periodic orbit remained stable, the formation of an infinitely large sequence of coexisting sinks appears feasible. However, so far, we did not analyze the evolutions of the invariant manifolds of the boundary saddles. Since the homoclinic tangency is a necessary criterion towards identification of these sinks as Newhouse sinks, we investigate the manifold evolutions in this paper and present some evidence that would suggest the birth of Newhouse sinks in a self-similar bifurcation structure. We consider the Toda oscillator model of the class-B lasers [20]:

$$\ddot{\Phi}+\alpha\dot{\Phi}+(1-m\cos\omega\tau)(\exp\Phi-1)=m\frac{\sqrt{D_u^2+\omega^2\Omega^2}}{D_u-1}\cos\left(\omega\tau+\tan^{-1}\frac{\omega\Omega}{D_u}\right), \tag{1}$$

where Φ represents the laser intensity (in logarithmic transformed scale). We consider a low dissipative case of the Toda oscillator ($D_u=2$, $\Omega=122.474$, $\alpha\equiv D_u/\Omega\cong 0.016$)

[2]By ''n tupling'' ($n>2$) we imply the birth of a period n-tupled saddle node in the neighboring phase space of a given stable periodic orbit.

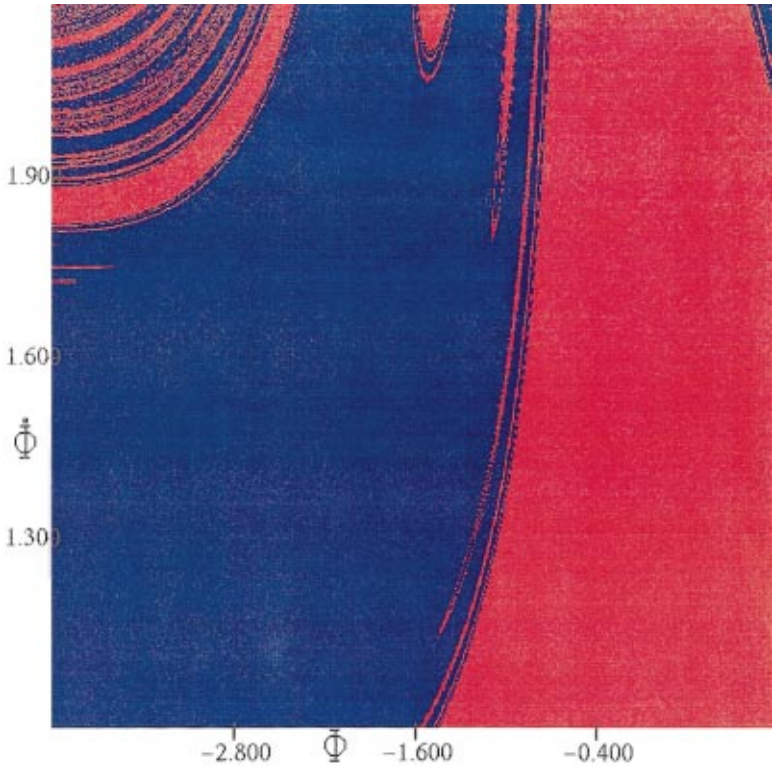

FIG. 2. (Color) Past homoclinic tangency, the period-1 basin (red) appears in fine scale within the period-3 basin (blue). $\omega=2.5$ and $m=0.005$. Φ along horizontal axis and $\dot{\Phi}$ along vertical axis. The features have some similarity with Fig. 1(b).

and neglect the nonlinear damping term from the oscillator equation of Ref. [20]. Henceforth, by ''period-n, (un)stable manifold'' we imply the (un)stable manifold of the period-n boundary saddle. We investigate the birth of secondary Newhouse sinks in the neighboring parameter space of the homoclinic tangency of the period-3 invariant manifolds in a period-3 subharmonic resonance region.

First, the driving frequency is kept constant at $\omega=2.5$ and the driving parameter m is increased as a control parameter. At a certain value of m ($m\cong 0.00474$), we observe the first homoclinic tangency. In Fig. 1 we show the scenario just after the first homoclinic tangency where the closure of the red component of the period-3 unstable manifold is a subset of the closure of the blue component.[3] Similarly, the closure of magenta component of the period-3 stable manifold is a subset of the closure of the maroon component. Past homoclinic tangency, an infinitely large number of tongues of the stable manifold (both the components) enter into the basin, previously occupied by period-3. The space within these tongues (i.e., within the components of the stable manifold), belongs to the period-1 basin. These tongues become thinner, longer, and folded, as it accumulates, along the stable manifold. Such a scenario may be seen in Fig. 2 which illustrates the basins of period-3 (blue) and of period-1 (red) at $m=0.005$.[4] One can very well notice the stretching and folding of the red tongues within the blue basin. As expected, the red tongues are becoming thinner along the boundary between red and blue basins.[5]

Past homoclinic tangency, we have observed a series of secondary Newhouse sinks around the stable period-3 orbit (Fig. 3). These sinks undergo sequence of period doubling whose parameter space representatives are some bifurcation substructures within the period-3 bifurcation structure. In plot 3(a), we show a few bifurcation curves of some of these substructures. The curve *a* denotes the period-3 saddlenode bifurcation and the curve *b* denotes the bifurcation curve for homoclinic tangency.[6] Prior to period doubling (period 3 $\rightarrow$6) [shown by curve (c)], we have observed a series of n tuplings around period-3 node, after homoclinic tangency. For instance, the curves *d*, *e*, and *f* denote respectively the period-9, -12, and -15 saddle node bifurcations. It seems that by increasing the driving parameter m at constant driving frequency, an infinite sequence of such n-tupled saddle nodes will appear around the stable period-3 after the tangency. The quotient of the periodicity of such saddle nodes and of

[3]The red component is not as clearly visible in Fig. 1(a) as the blue component, after crossing the maroon stable manifold, remains in the close vicinity of the red unstable component. The red component is more clearly shown in (d).

[4]Fig. 2, and later Figs. 9 and 11 are prepared by integrating (600×600) trajectories of Eq. (1) within the phase space, shown in these figures.

[5]Under such circumstances, following Grebogi *et al.* [29], we may state that the basin boundary would become complex similar to a fractal.

[6]I.e., if the driving parameter m is increased to intersect curve b from below, the period-3 invariant manifolds undergo first tangency.

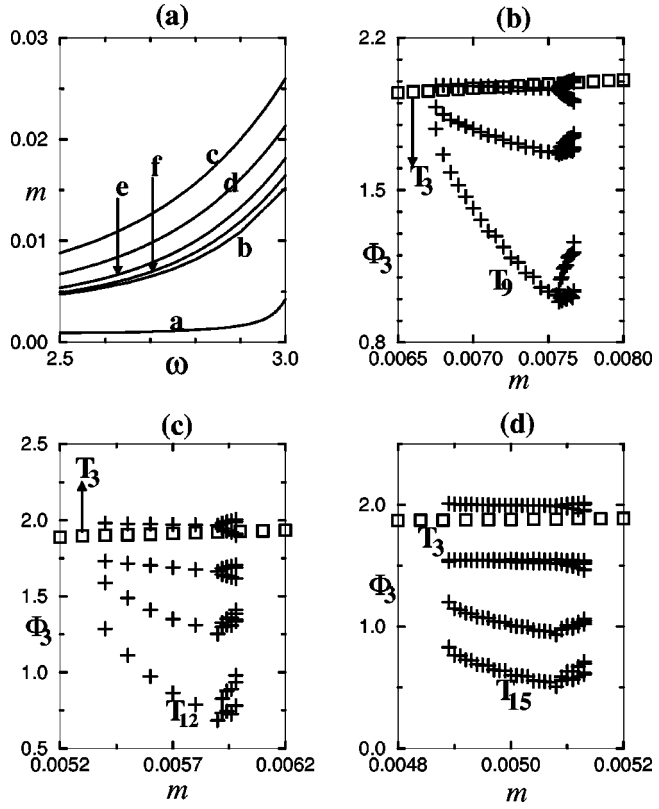

FIG. 3. Homoclinic tangency and the first-order secondary Newhouse sinks, born in period tripling, quadrupling, and pentupling processes, around the period-3 sink. (a) The associated bifurcation substructures within the period-3 bifurcation structure. The bifurcation curves *a*, *d*, *e*, and *f* denote respectively the period-3, -9, -12, and -15 saddle node bifurcations. The bifurcation curves *b* and *c* denote, respectively, the homoclinic tangency and the period doubling ($3\rightarrow 6$). In plots (b)–(d), respectively, the period-9, -12, and -15 branches (plus signs) have been shown to coexist around the period-3 orbit (rectangles); $\omega = 2.5$.

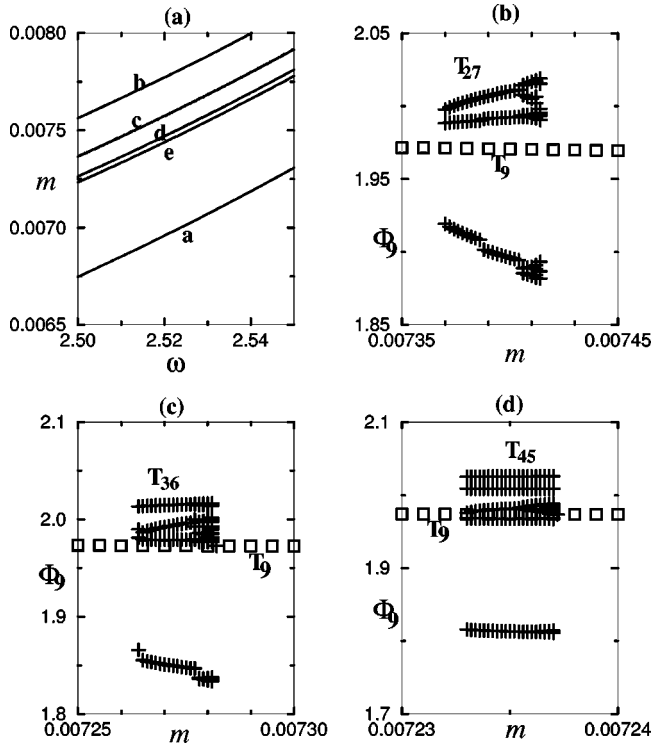

FIG. 4. Second-order secondary Newhouse sinks, born in period tripling, quadrupling, and pentupling, around the period-9 sink. (a) The associated second-order bifurcation substructures within the period-9 substructure. The bifurcation curves *a*, *c*, *d*, and *e* denote, respectively, the period-9, -27, -36, and -45 saddle node bifurcations. The bifurcation curve b denotes the period doubling ($9 \rightarrow 18$). In plots (b)–(d), respectively, the period-27, -36, and -45 branches (plus signs) have been shown to coexist around period-9 orbit (rectangles); $\omega = 2.5$.

period-3 constitute an infinite sequence of integers (viz., $\ldots,6,5,4,3$). These saddle and nodes may be identified as the first-order secondary Newhouse orbits around the primary Newhouse sink of period 3. As the driving parameter is swept, each sink constitutes a period doubling cascade (secondary cascade). In Figs. 3(b), 3(c), and 3(d), respectively, the period-9, -12, and -15 branches have been shown to coexist around period-3 orbit. In Figs. 3 and the following figures, Φ_n represents the asymptotic Φ, stroboscopically mapped with a sampling interval $2n\pi/\omega$; T_n denotes a period-*n* branch. As one may notice from Figs. 3, these secondary cascades appear in sequence and exist in separate intervals in the control parameter space.

Such a series of *n* tuplings appears to recur in a self-similar manner, giving birth of higher order secondary Newhouse sinks. Each sink similarly constitutes its own secondary cascade whose parameter-space representative is a higher order bifurcation substructure. For instance, in Fig. 4 we show a similar substructure formation around the period-9 node. In Fig. 4(a), the curves *a* and *b* denote the period-9 saddle node bifurcation and the period doubling ($9\rightarrow 18$). The curves *c*, *d*, and *e* denote, respectively, the period-27, -36, and -45 saddle node bifurcations. In Figs. 4(b)–4(d), we show the associated higher-order secondary cascades, namely, the period-27, -36, and -45 branches, respectively. Each secondary cascade coexists with the period-9 node of the period-9 branch. These branches appear in separate windows in the parameter space. Each window is a subinterval of the window where period-9 remains stable. Notice that the period-9 orbit itself coexists around the period-3 which, in turn, is located around period-1. Therefore, the periodic orbits from each secondary branch coexist with period-9, -3, and -1 orbits. In other words, if the control parameter value belongs to any one of these windows, one may find a sequence of three Newhouse sinks coexisting with period 1. In Fig. 5, we show a similar scenario around the period-12 orbit of the period-12 branch. In Fig. 5(a), the curves *a* and *b* denote, respectively, the period-12 saddle node bifurcation and period doubling ($12\rightarrow 24$). The curves *c*, *d*, and *e* denote, respectively, the period-36, -48, and -60 saddle node bifurcations. In Figs. 5(b)–5(d), we show the associated higher order secondary cascades, viz., the period-36, -48, and -60 branches. Each branch coexists in the phase space with the period-12, -3, and -1 sinks. In Fig. 6, we show another similar scenario around the period-15 node. In Fig. 6(a), the curves *a* and *b* denote, respectively, the period-15 saddle node bifurcation and period doubling ($15\rightarrow 30$). The curves *c* and *d* denote the period-45, and period-60 saddle node bifurcations. In Figs. 6(b)–6(c), we show the period-45 and -60 branches, each of them coexisting with the period-15, -3, -1 sinks. Such a scenario appears to be recurrent, as we show

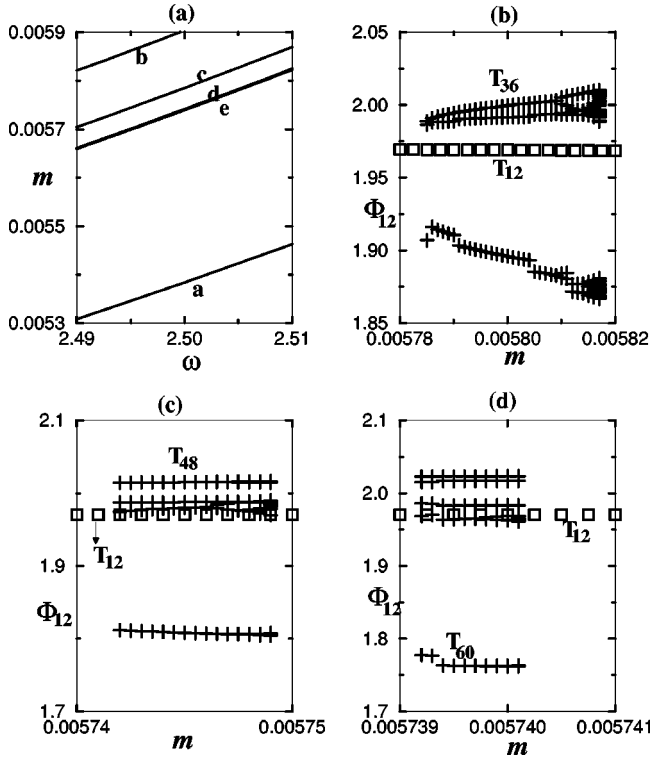

FIG. 5. Second-order secondary Newhouse sinks, born in period tripling, quadrupling, pentupling around the period-12 sink. (a) The associated second-order bifurcation substructures within the period-12 bifurcation substructure. The bifurcation curves *a*–*e* denote, respectively, the period-12, -36, -48, and -60 saddle node bifurcations. As we have to show all the curves simultaneously, the curves *d* and *e* could not be shown with better resolution. The bifurcation curve *b* denotes the period doubling ($12\rightarrow24$). In plots (b)–(d), respectively, the period-36, -48, and -60 branches (plus signs) have been shown to coexist around period-12 orbit (rectangles); $\omega=2.5$.

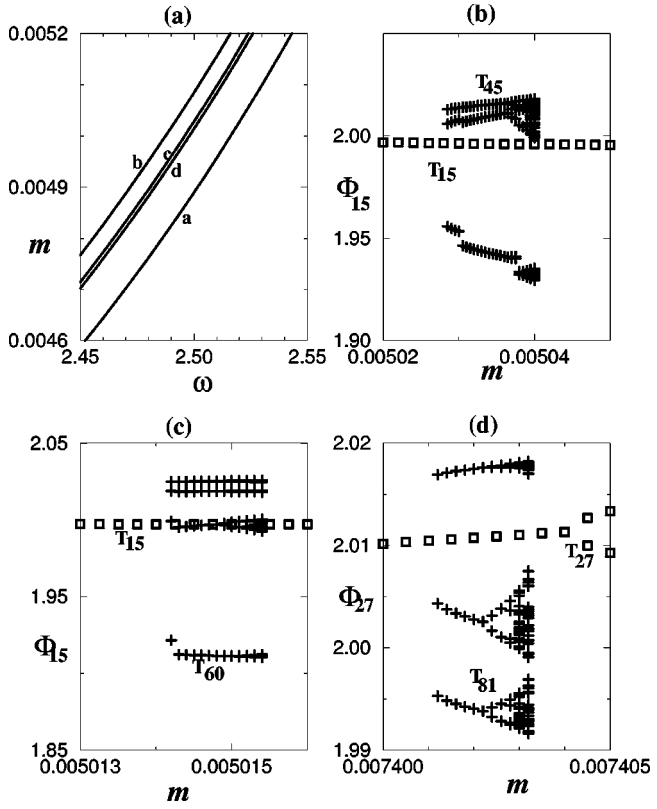

FIG. 6. Second-order secondary Newhouse sinks, born in period tripling, quadrupling, around period-15 sink. (a) The associated second-order bifurcation substructures within the period-15 bifurcation substructure. The bifurcation curves *a*, *c*, and *d* denote respectively the period-15, -45, and -60 saddlenode bifurcations. The bifurcation curve *b* denotes the period doubling ($15\rightarrow30$). In plots (b) and (c), respectively, the period-45, and -60 branches (plus signs) have been shown to coexist around period-15 orbit (rectangles); $\omega=2.5$. (d) period-81 branch (plus signs), born in period tripling around period-27 (rectangles) of period-27 branch; $\omega=2.5$.

in the next plot [Fig. 6(d)] where the period-81 secondary cascade coexists with the period-27 sink of the period-27 branch. Thus, if the control parameter value belongs to the window of period-81 branch, one may find a set of four Newhouse sinks, coexisting with period-1. Proceeding further in a similar manner, one may argue that in some subintervals within the window of period-81, more number of higher order secondary Newhouse sinks may be observed. The limit of such a sequence could be infinitely large.

These observations suggest the birth of Newhouse sinks in a self-similar bifurcation structure formation. In the next schematic (Fig. 7), we illustrate these features. Figure 7(I) shows three first order bifurcation substructures within the period-3 bifurcation structure in $(m-\omega)$ space. The lines *a*, *b*, and *c* denote, respectively, the period-3 saddle node bifurcation, the homoclinic tangency, and the period doubling ($3\rightarrow6$). The hatched bands *d*, *e*, and *f* denote the first order substructures, born in the process of period tripling, quadrupling, and pentupling respectively. If such a ''composite structure'' (i.e., the superposition of the period-3 bifurcation structure and the set of first-order substructures) is probed with *m* as the control parameter, each stable orbit of the period-3 branch (P) would be typically found to be associated with an infinite series of secondary cascades. Such a situation is illustrated schematically in Fig. 7(II). The secondary cascades, born around the orbit of period $3\times2^{p_1-1}$ ($p=1,2,3,\ldots$), in period tripling, quadrupling and pentupling, are respectively denoted by Tp, Qp, Pp. Each cascade is shown by one of its components. The boundary saddles are shown by the segmented lines. For some numerical evidences, we may refer back to Figs. 3. Each secondary Newhouse sink plays the same role as the primary Newhouse sink period 3. In Fig. 7(III), the bifurcation curves *a* and *b* denote, respectively, the period-$3n$($n=3,4,5,\ldots$) saddlenode bifurcation, and the period doubling ($3n\rightarrow6n$). The hatched bands *c*, *d*, and *e* denote the second order substructures, born in the process of period tripling, quadrupling, and pentupling respectively. If such a composite first-order substructure (say a period-$3n$ bifurcation substructure) is probed with *m* as the control parameter, each stable orbit of the period-$3n$ branch (P') would be found to be associated with an infinite series of higher order secondary cascades. Such a situation is illustrated schematically in Fig. 7(IV). The secondary cascades, born around the orbit of period $3n\times2^{p-1}$, in period tripling, quadrupling and pentupling, are respectively denoted by $T'p$, $Q'p$, $P'p$. Each cascade is shown by one of its components. The boundary

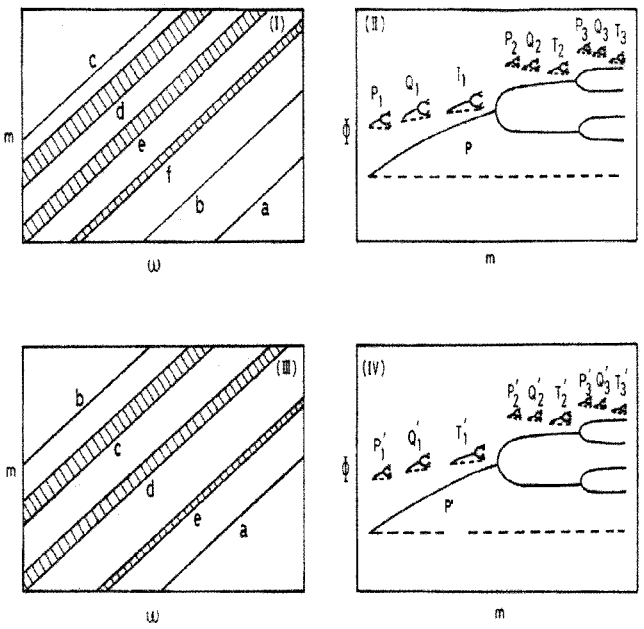

FIG. 7. The schematic illustration of homoclinic tangency within the self-similar bifurcation structure. (I) The lines *a*–*c* represent the bifurcation curves for, respectively, the period-3 saddle node bifurcation, the homoclinic tangency of the period-3 invariant manifolds, and the period doubling $(3\rightarrow 6)$. The hatched bands *d*, *e*, and *f* represent the substructures, born in period tripling, quadrupling, and pentupling, respectively. (II) A series of secondary cascades in association with the period-3 branch (P). The secondary cascades, born around the stable orbit of period $3\times 2^{p-1}$ $(p=1,2,3)$ in period tripling, quadrupling, and pentupling are respectively denoted by T_p, Q_p, P_p. (III) The lines (a) and (b) represent the bifurcation curves for the period-$3n$ saddlenode bifurcation, and the period doubling $(3n\rightarrow 6n)$, respectively. The hatched bands *c*–*e* represent the substructures, born in period tripling, quadrupling, and pentupling, respectively. (IV) A series of secondary cascades in association with the period-$3n$ branch (P'). The secondary cascades born around the stable orbit of period $3n\times 2^{p-1}$ $(p=1,2,3)$ in period tripling, quadrupling, and pentupling are respectively denoted by T_p', Q_p', P_p'.

saddles are shown by the segmented lines. For some numerical evidences, we may refer to Figs. 4–6. These processes are expected to continue in a self-similar manner, giving birth to a hierarchy of coexisting secondary Newhouse sinks. One common feature, appearing from these observations, is that each higher order secondary cascade exists in a parameter window which is a subinterval of the window of the original cascade. Let w_n denote the window of the a period-n sink Also, let W_{3n}, W_{4n}, and W_{5n} denote respectively the windows where the secondary cascades T_n, Q_n, and P_n exist. We find that $W_{pn}\subset w_n$; $p=3,4,5,\ldots$. Thus, in the window where the period-3 orbit of period-3 branch exists, there could be an infinite series of subwindows for the first-order secondary cascades. Again, within the window of each periodic orbit from each of these first-order secondary cascades, there may be a new series of smaller subintervals where the second order cascades will appear. These processes are likely to go on in a self-similar manner. Therefore, one may expect that an infinitely large sequence of coexisting Newhouse sinks will exist apparently for an infinitely large number of parameter values within the window where the period-3 branch exists.

Our results also suggest that the windows of a given order secondary Newhouse sinks obey certain inequalities. For instance, the largest window belongs to the cascade born in period tripling and the window becomes smaller as we move on to period quadrupling, pentupling, and so on. In mathematical notation, $|W_{3n}|>|W_{4n}|>|W_{5n}|\cdots$. As n increases, the windows become smaller but follow the same inequality.

Next we bring attention to the basins of the Newhouse sinks. Eschenazi *et al.* [30] have earlier observed that the basins of the primary Newhouse sinks undergo reorganization to indicate and finally accommodate the new basin. We study here the basin formation of the secondary Newhouse sinks and the associated invariant manifolds of the secondary Newhouse saddles. In Fig. 8, we show a case after the birth of period-9 saddlenode around the period-3 sink. Our observations suggest that the closure of period-9 unstable manifold (dark and light green points) is a subset of the closure of the period-3 unstable manifold [dark blue points in plot (a)]. The period-9 stable manifold [black and orange points in Fig. 8(b)] moves around within the period-3 basin, defined by the period-3 stable manifold [red and yellow points in Fig. 8(a)]. The stable manifold of period-9 saddle indicates the basin of the period-9 sink, depleted from the basin of period-3 sink. In the remote region where the period -3 and -9 stable manifolds coexist densely, one would find the presence of the period-9, -3, and -1 basins in a fine scale. In Fig. 9, we show the associated computed basins of attraction of period-1, -3, and -9 nodes. The three fingers of period-9 basin (dark blue) appear within the period-3 basin (light blue). Away from the central region, the union of period-9 and -3 basins twist and stretch around. Thus, a secondary Newhouse orbit, and its basin appear within the basin of the original primary Newhouse sink itself, in some sense implying a ''genealogical link'' between the original primary Newhouse sink and the secondary Newhouse orbits.

Such a subdivision of the basin appears to repeat at every stage of period n tupling. For instance, Figs. 10 illustrate the invariant manifolds of period-3, -9, and -27 saddles shortly after the birth of period-27 saddle node around period-9 node. By comparing the plots (a) and (b), one may notice that the period-9 unstable manifold remains in the close vicinity of green period-3 unstable manifold, and even follows it to the period-1 node [near the right bottom corner of plots (a) and (b)]. Thus their closures have become identical. In the plot (c), we show a closeup around the period-9 node at the center of the black points. It is apparent that closure of period-27 unstable manifold is a subset of closure of period-9 unstable manifold. The period-27 stable manifold moves within the period-9 basin, determined by the period-9 stable manifold. Thus the period-27 basin is created by depleting a portion of the period-9 basin. The overall phase space may be broadly categorized into two regions: (i) the core regions around period-1, -3, -9, and -27 sinks, (ii) the remote regions where the stable manifolds coexist densely. For instance, the dense coexistence of the period-3, -9, and -27 stable manifolds indicate the presence of fine layers of the period-1, -3, -9, and -27 basins. In Fig. 11, we show the associated computed basins of attraction of period-1, -3, -9, and -27 nodes. By comparing with Fig. 10(c), one can find a good agreement. Eschenazi *et al.* [30] have earlier observed

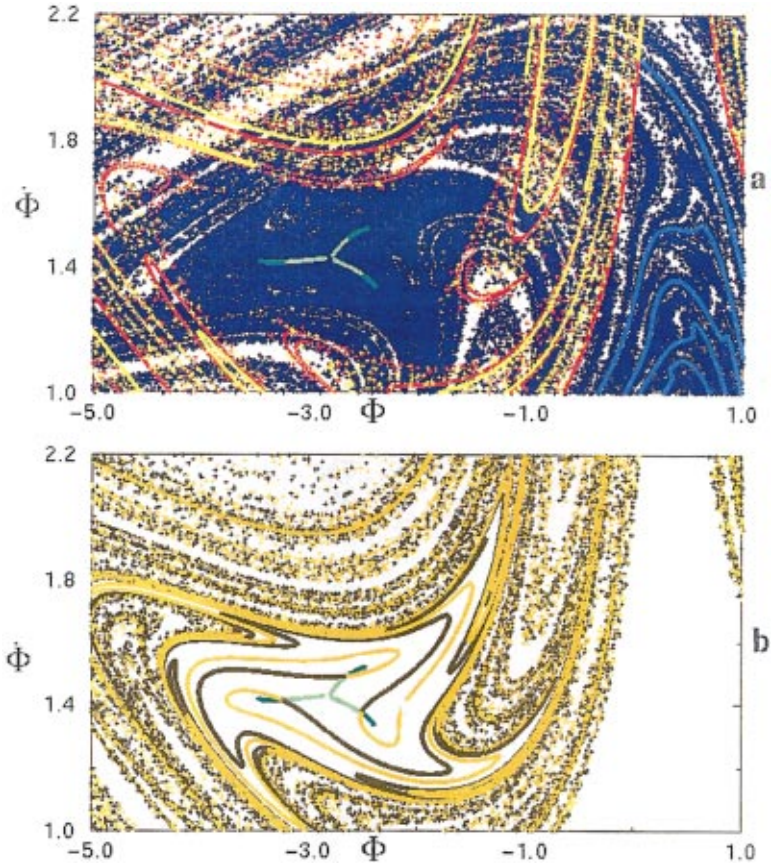

FIG. 8. (Color) The formation of period-9 basin within the period-3 basin. $\omega=2.5$ and $m=0.00676$. (a) Red and yellow points show two components of period-3 stable manifold. Dark and light blue points show two components the period-3 unstable manifold. The dark and light green points at the central region show two components of the period-9 unstable manifold. (b) The black and orange points show two components of the period-9 stable manifold. Dark and light green points show two components of period-9 unstable manifold.

that as a periodic sink undergoes sequence of period doubling, the basin itself gets split into as many parts as the stage of period doubling. We illustrated here that the basin of a primary Newhouse sink may undergo similar depletion (or splitting) due to the creation of secondary Newhouse sinks. The higher-order secondary sinks will have a smaller basin. Thus, as the system enters into the hyperfine bifurcation structures, more number of secondary sinks would appear. However, the basins of these secondary sinks will be smaller and remain intertwined with the basins of the lower-order

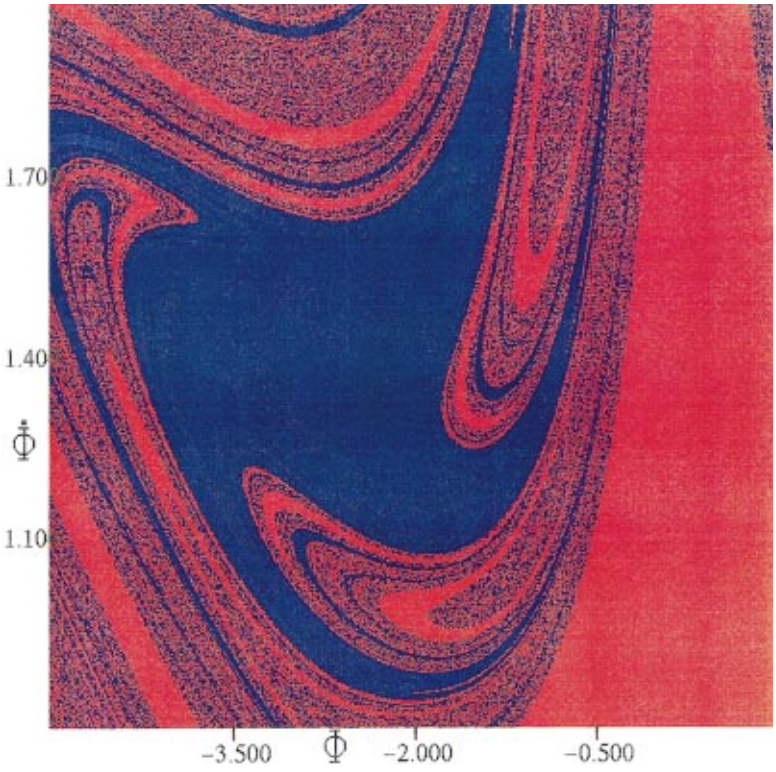

FIG. 9. (Color) The period-9 basin (dark blue) appears within the period-3 basin (blue). The red basin belongs to period 1. $\omega=2.5$ and $m=0.00676$. $\dot{\Phi}$ along the vertical axis and Φ along the horizontal axis. The period-9 basin is created by depletion of a part of the period-3 basin. The stable manifolds, which demarcate the basin boundaries, may be seen in Fig. 8.

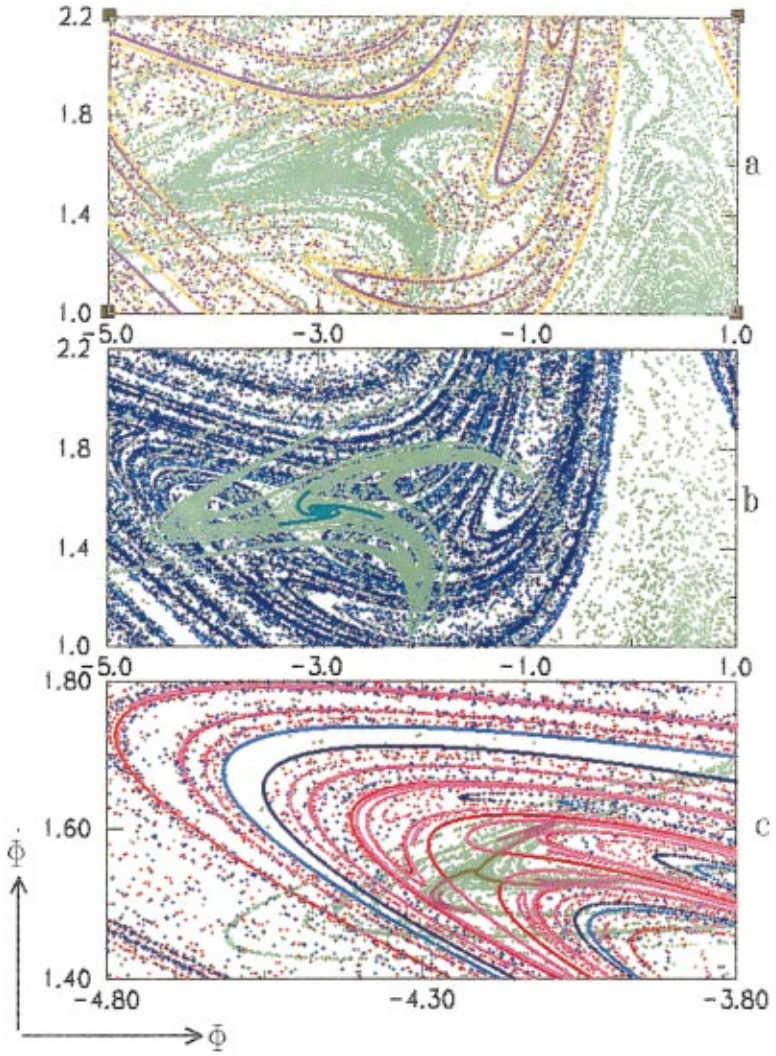

FIG. 10. (Color) The formation of period-27 basin after period tripling around period-9. $\omega = 2.5$ and $m = 0.0074$. (a) The green points show one component of the period-3 unstable manifold. The orange and Indigo points denote two components of the period-3 stable manifold. (b) The dark and light green points show two components of the period-9 unstable manifold. The dark and light blue points show two components of the period-9 stable manifold. (c) The red and magenta points show two components of the period-27 stable manifold. The black and maroon points show two components of the period-27 unstable manifold. Rest are in the same convention as in (b).

secondary sinks.

In these analyses, we focused only on sequence of period tripling as a typical example. Notice that all the n tuplings behave in a very similar manner, as evident from the figures (Figs. 3–6), and from our earlier paper [20]. We believe that similar inference may also be obtained from any case of period n tupling and its heterogeneous combinations, i.e., in stead of a sequence of period tripling, one may consider a sequence of several n tuplings. Therefore, we may conjecture the following points with regard to the basins of secondary Newhouse sinks.

(i) The unstable manifold of a secondary Newhouse saddle connects the primary Newhouse sink on one side and the secondary Newhouse sink on the other side. The stable manifold of a secondary Newhouse saddle moves within the basin of corresponding primary Newhouse sink, determined by the stable manifold of the primary Newhouse saddle. Thus the basin of a secondary Newhouse sink is formed by depleting the basin of the respective primary Newhouse sink. The basin of the secondary sink always remains intertwined with the basin of the primary sink. The features will be similar in the case of creation of higher order secondary Newhouse sinks.

(ii) In each case of period n tupling, say around period-$3p$ ($p \geq 1$), the period-$3pn$ saddle node appears in the closure of the period-$3p$ unstable manifold. Past such bifurcation, the closure of the period-$3pn$ unstable manifold remains a subset of the closure of period-$3p$ unstable manifold. In each case of period n tupling, say around period-$3p$ ($p = 3,4,5, \ldots$), the closure of the unstable manifold of period-$3p$ saddle is identical to the closure of the period-3 unstable manifold.

(iii) In each case of period n tupling, say around period-$3p$ ($p > 1$), there will be heteroclinic crossing between the stable manifolds of period-$3pn$ saddle and the unstable manifold of period-$3p$ saddle. Since, the closure of the unstable manifold of period-$3p$ is identical to the closure of period-3 saddle, there will be similar heteroclinic crossings between the stable manifolds of period-$3pn$ saddle and the unstable manifold of the period-3 saddle as well.

To conclude, the following features of the periodically driven Toda oscillator have been observed numerically. Sequence of subharmonic resonances lead to the birth of sequence of primary Newhouse orbits (sinks and saddles). As a control parameter is swept in the neigboring parameter space of the homoclinic tangency of the invariant manifolds of a primary saddle, first-order secondary Newhouse sinks are born around the corresponding primary Newhouse sink in a series of period n-tupling processes. A series of higher order secondary Newhouse sinks are born in similar n-tupling processes, in a recurrent manner, around those first-order sec-

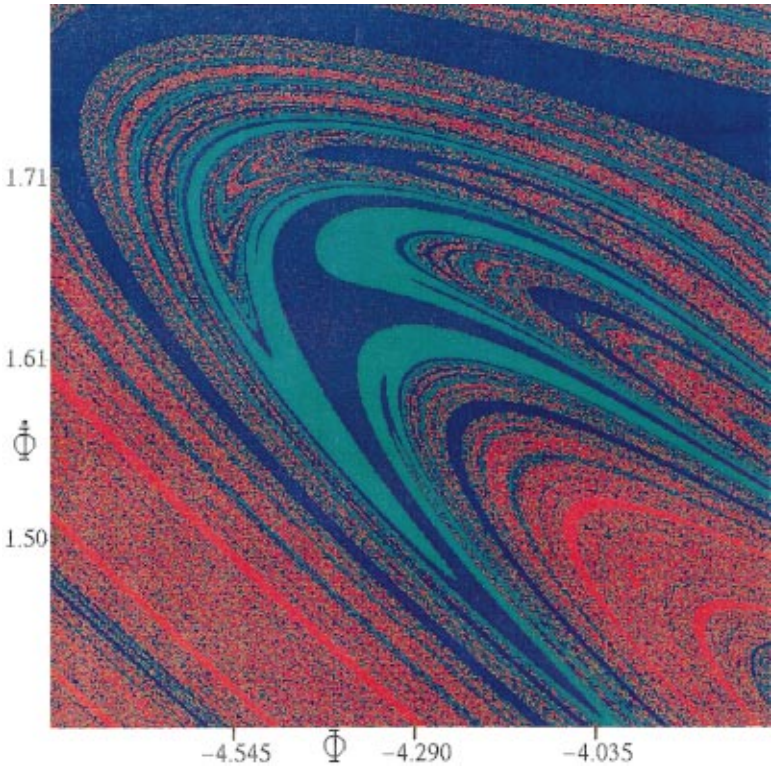

FIG. 11. (Color) Coexistence of the basins of Newhouse sinks after period tripling around period 9. $\omega = 2.5$ and $m = 0.0074$. $\dot{\Phi}$ along vertical axis and Φ along horizontal axis. Red, light blue, dark blue, and green basins belong to, respectively, period-1, -3, -9, and -27 sinks. Some idea about the stable manifolds, which demarcate the basin boundaries, may be obtained from Fig. 10.

ondary sinks, constituting a self-similar bifurcation structure in the parameter space. The secondary cascade from each higher order secondary Newhouse sink exists within a small subinterval of the control parameter window where the lower-order secondary Newhouse sinks exists. The unstable manifold of a secondary Newhouse saddle connects the primary Newhouse sink on one side and the secondary Newhouse sink on the other side. The stable manifold of a secondary Newhouse saddle moves within the basin of the respective primary Newhouse sink. Thus the basin of the secondary Newhouse sink is formed by depleting the basin of the primary Newhouse sink. The features are recurrent in the case of creation of higher-order secondary Newhouse sinks. Therefore, the higher-order secondary sinks appear with progressively smaller basins intertwined with the basins of lower-order secondary sinks.

The author is sincerely grateful to Dr. N. Venkatramani and Dr. K. Dasgupta for useful comments. He thanks Dr. A. N. Pisarchik, Stepanov Institute of Physics, Minsk, Belarus for bringing to notice some important references. He also finds pleasure to acknowledge the help from Phool Chand and Rajesh in color graphics and computations in ANUPAM parallel processing network in Computer Center.

[1] N.K. Gavrilov and L.P. Shilnikov, Math. USSR Sbornik **17**, 467 (1972); **19**, 139 (1973).
[2] C. Robinson, Commun. Math. Phys. **90**, 433 (1983).
[3] J. Maurer and A. Libchaber, J. Phys. (France) Lett. **41**, 515 (1980).
[4] F.T. Arecchi and P. Lisp, Phys. Rev. Lett. **49**, 94 (1982); **50**, 1328 (1983).
[5] F.T. Arecchi, R. Meucci, G. Puccioni, and J.R. Tredicce, Phys. Rev. Lett. **49**, 1217 (1982).
[6] E. Brun, B. Derighetti, D. Meier, R. Holzner, and M. Ravani, J. Opt. Soc. Am. B **2**, 156 (1985); J.R. Tredicce, F.T. Arecchi, G.P. Puccioni, A. Poggi, and W. Gadomsky, Phys. Rev. A **34**, 2073 (1986).
[7] D. Dangoisse, P. Glorieux, and D. Hennequin, Phys. Rev. Lett. **57**, 2657 (1986); D. Dangoisse, P. Glorieux, and D. Hennequin, Phys. Rev. A **36**, 4775 (1987).
[8] H.G. Solari, E. Eschenazi, R. Gilmore and J.R. Tredicce, Opt. Commun. **64**, 49 (1987).
[9] A.N. Pisarchik and B.K. Goswami, Phys. Rev. Lett. **84**, 1423 (2000).
[10] T. Kapitaniak, J. Brindley, and L. Kocarev, Geophys. Res. Lett. **22**, 1257 (1995).
[11] J.M.T. Thompson and H.B. Stewart, *Nonlinear Dynamics and Chaos* (Wiley, Chichester, 1986).
[12] J. Curry, Commun. Math. Phys. **68**, 129 (1979).
[13] John Guckenheimer and Philip Holmes, *Nonlinear Oscillations, Dynamical Systems, and Bifurcation of Vector Fields* (Springer Verlag, New York, 1983).
[14] F.T. Arecchi, R. Badii, and A. Politi, Phys. Rev. A **32**, 402 (1985).
[15] W. Szemplin'ska-Stupnicka, in *Chaotic Motions in Nonlinear Dynamical Systems*, CISM No. 298, W. Szemplin'ska-Stupnicka, G. Iooss, and F.C. Moon (Springer-Verlag, Wien, 1988), p. 51.
[16] R. Meucci, A. Poggi, F.T. Arecchi, and J.R. Tredicce, Opt. Commun. **65**, 151 (1988).
[17] B.K. Goswami, Int. J. Bifurcation Chaos Appl. Sci. Eng. **5**, 303 (1995).

[18] B.K. Goswami, Opt. Commun. **122**, 189 (1996).
[19] B.K. Goswami, Int. J. Bifurcation Chaos Appl. Sci. Eng. **12**, 2691 (1997).
[20] B.K. Goswami, Phys. Lett. A **245**, 97 (1998).
[21] M. Surgent III, M.O. Scully, and W.E. Lamb, Jr., *Laser Physics* (Addision-Wesley, London, 1974), Chap. 8, pp. 96-113.
[22] H. Haken, Phys. Lett. **53A**, 77 (1975).
[23] B.K. Goswami and D.J. Biswas, Phys. Rev. A **36**, 975 (1987); V.N. Chizhevsky, R. Corbalán, and A.N. Pisarchik, Phys. Rev. E **56**, 1580 (1997); A.N. Pisarchik and R. Corbalán, *ibid.* **59**, 1669 (1999).
[24] U. Feudel, C. Grebogi, B.R. Hunt, and J.A. Yorke, Phys. Rev. E **54**, 71 (1996).
[25] S.E. Newhouse, Topology **12**, 9 (1974); Pub. Math. IHES **50**, 101 (1979) *Lectures on Dynamical Systems.* Vol. 8 of *Progress in Mathematics* (Birkhaüser, Boston, 1980).
[26] Laura Tedeschini-Lalli and James A. Yorke, Commun. Math. Phys. **106**, 635 (1986).
[27] Y.-C. Lai, C. Grebogi, J.A. Yorke, and I. Kan, Nonlinearity **6**, 779 (1993).
[28] I. Kan, H. Kocak, and J.A. Yorke, Physica D **83**, 313 (1995).
[29] C. Grebogi, E. Ott, and J.A. Yorke, Physica D **24**, 243 (1987).
[30] E. Eschenazi, H.G. Solari, and R. Gilmore, Phys. Rev. A **39**, 2609 (1989).
[31] G.L. Oppo and A. Politi, Z. Phys. B: Condens. Matter **59**, 111 (1985).
[32] B.K. Goswami, Phys. Lett. A **190**, 279 (1994).